Environmental Technology
Publication details, including instructions for authors and subscription information:
http://www.tandfonline.com/loi/tent20

Potential use of calcareous mudstones in low hydraulic conductivity earthen barriers for environmental applications

T. B. Musso [a b], F. M. Francisca [c b], M. E. Parolo [a] & K. E. Roehl [d]

[a] Departamento de Geología y Petróleo, Facultad de Ingeniería, Universidad Nacional del Comahue, Buenos Aires, Argentina

[b] CONICET: Consejo Nacional de Investigaciones Científicas y Técnicas

[c] Departamento de Construcciones Civiles, Universidad Nacional de Córdoba, Córdoba, Argentina

[d] Institute of Applied Geosciences, Technische Universität Darmstadt, Darmstadt, Germany

Accepted author version posted online: 04 Feb 2013.Version of record first published: 28 Feb 2013.

Environmental Technology, 2013
http://dx.doi.org/10.1080/09593330.2013.772660

Potential use of calcareous mudstones in low hydraulic conductivity earthen barriers for environmental applications

T.B. Musso[a,b]*, F.M. Francisca[c,b], M.E. Parolo[a] and K.E. Roehl[d]

[a]*Departamento de Geología y Petróleo, Facultad de Ingeniería, Universidad Nacional del Comahue, Buenos Aires, Argentina;* [b]*CONICET: Consejo Nacional de Investigaciones Científicas y Técnicas;* [c]*Departamento de Construcciones Civiles, Universidad Nacional de Córdoba, Córdoba, Argentina;* [d]*Institute of Applied Geosciences, Technische Universität Darmstadt, Darmstadt, Germany*

(*Received 11 July 2012; final version received 27 January 2013*)

Earthen layers play a significant role in isolating contaminants in the subsurface, controlling the migration of contaminant plumes, and as landfill liners and covers. The physical, chemical and mineralogical properties of three calcareous mudstones from the Jagüel and Roca formations in North Patagonia, Argentina, are evaluated to determine their potential for the construction of liners. These mudstones were deposited in a marine environment in the Upper Cretaceous–Paleocene. The tested specimens mainly comprise silt and clay-sized particles, and their mineralogy is dominated by a smectite/illite mixed layer (70–90% Sm) and calcite in smaller proportion. Powdered mudstone samples have little viscosity and swelling potential when suspended in water. The hydraulic conductivity of compacted mudstones and sand–mudstone mixtures is very low (around 1–3 $\times 10^{-10}$ m/s) and in good agreement with the expected hydraulic behaviour of compacted earthen layers. This behaviour can be attributed to the large amount of fine particles, high specific surface and the close packing of particles as confirmed by scanning electron microscope analysis. The tested materials also show a high cation exchange capacity (50–70 cmol/kg), indicating a high contaminant retardation capability. The calcareous mudstones show satisfactory mineralogical and chemical properties as well as an adequate hydraulic behaviour, demonstrating the potential use of these materials for the construction of compacted liners for the containment of leachate or as covers in landfills. These findings confirm the potential usage of marine calcareous mudstones as a low-cost geomaterial in environmental engineering projects.

Keywords: mudstones; sand–mudstone mixtures; containment barriers; hydraulic conductivity; liners

1. Introduction

Clay-rich materials, especially bentonites, are frequently used in civil engineering, petroleum industry and environmental applications. The most common purposes include sealants and liners in dams, slurries, landfills and surface impoundments [1,2]. Different types of barriers have been used to minimize leachate displacement and contaminant transport from waste disposal sites. In any case, the barrier performance depends on the composition and structure of the liner system installed.

The US Environmental Protection Agency guidance recommends the incorporation of a compacted clay layer for the liner and cover system in landfills [3]. Several alternatives, which include multiple layers and the inclusion of geosynthetic clay liners are also available. The compacted clay liner must be sufficiently thick to prevent hazardous constituent migration, while the cover function is to minimize the entry of rain water to the cells and to prevent the leakage of landfill gas. Bentonite and sand–bentonite mixtures are commonly used for this purpose, given that the hydraulic conductivity of this expandable material is noticeably lower than the value specified by current international regulations for the construction of liners ($k < 10^{-9}$ m/s) [4,5].

In many cases, it is difficult or costly to obtain geomaterials which have a good performance and long-term behaviour in liners. Therefore, it is advisable to search for a natural material or local soil that could be used in these applications, either in its natural state, or mechanically, chemically or physically enhanced or stabilized [6,7].

Mudstones represent the major constituents of sedimentary basins worldwide. They are low-permeability sedimentary rocks with a high sorption capacity; consequently, in the basins they form seals for hydrocarbon accumulations and act as aquitards, and also as chemical barriers [8,9]. In near-surface environments, they are important natural barriers which restrict leakage from waste disposal sites (such as radioactive facilities) [10–14]. Also, in their natural state, mudstones show significant spatial variability of physical properties, clay content and hydraulic conductivity [15,16]. However, there is poor understanding of the feasibility of outcropping mudstones material to be used as

*Corresponding author. Email: telma.musso@fain.uncoma.edu.ar

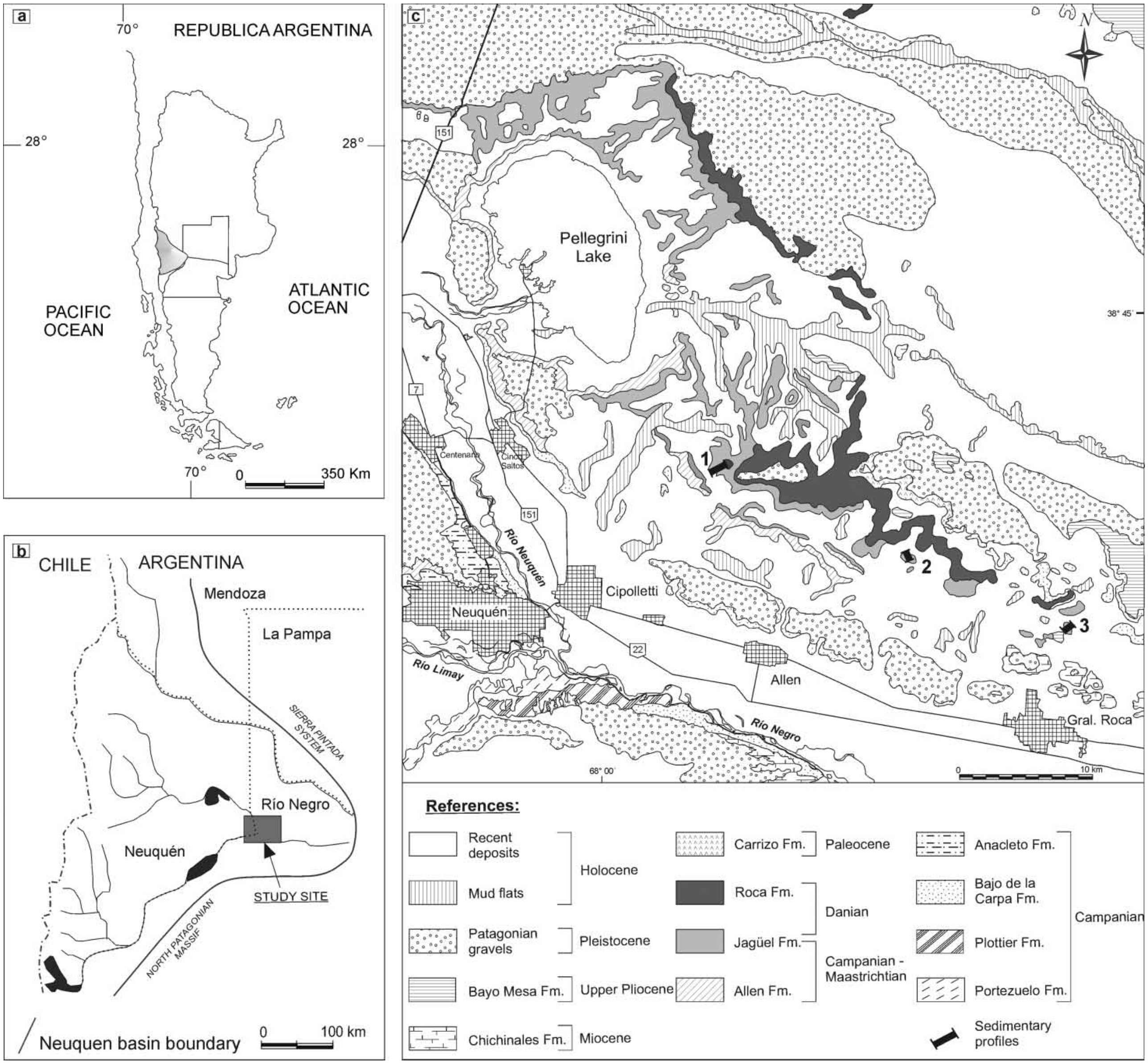

Figure 1. Location maps (a), (b) and geological map of the studied area. Modified from Espejo and Nieto [23] and Hugo and Leanza [24] (c). 1: Cerro Azul profile, 2: Cerro Tres Picos profile, 3: Este Puesto Lopez profile.

compacted clay liners, alone or in combination with other natural materials (soil or sand).

The aim of this study is to determine the most significant physical, chemical, mineralogical and hydraulic properties of three widely spread mudstones from North Patagonia Argentina, to evaluate the potential use of these materials for the construction of earthen barriers in environmental applications.

2. Geology of tested mudstones

The Neuquén Basin (Figure 1) is a sedimentary basin in western Argentina with deposits ranging in age from Late Triassic to Tertiary. Sediments were deposited in this basin in three sedimentary cycles: Jurásico, (Late Triassic–Late Jurassic), Ándico (Late Jurassic–Early Cretaceous) and Riograndico (Late Cretaceous–Paleocene) [17]. The uppermost Riográndico cycle includes the Malargüe Group represented in the study area by the Allen, Jagüel and Roca Formations [18]. The mudstones under analysis are part of the Jagüel and Roca formations. These formations are separated by a transitional boundary, and many authors consider both formations as part of the same sedimentary cycle [19].

Two siliciclastic and a carbonate lithofacies were identified in this area by analysing the physical properties and the age of the sediments (Figure 2): Maastrichtian grayish yellow calcareous mudstones, Danian olive gray

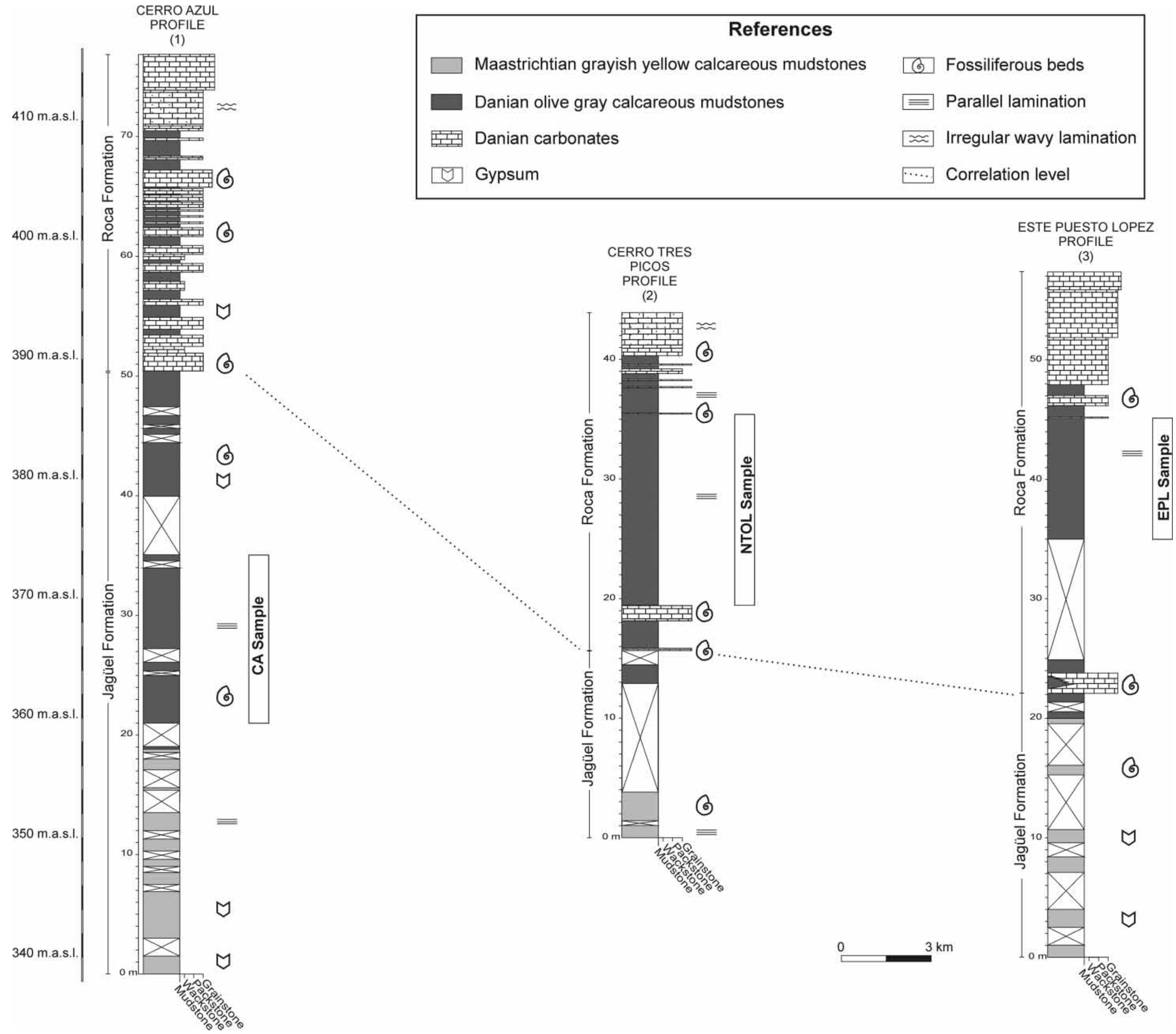

Figure 2. Sedimentary profiles showing the position of the sampled mudstones levels. Modified from Musso et al. [20].

calcareous mudstones, and Danian carbonates [20]. An outer shelf depositional setting was assigned to the Jagüel formation [19,21,22]. The Roca formation was formed in a shallow marine environment passing upwards to a sabkha [19].

3. Materials and methods

3.1. Tested samples

Representative samples were taken from Jagüel formation (identified as CA) and Roca formation (identified as NTOL and ETRO) outcrops as shown in Figure 2. The mudstones cover a flat-shaped highland area of around 1000 km^2 of the study area. In the field, the samples have the consistency of hard rock. Chunks of rocks were crushed, resulting in powdered mudstones that were used to determine their mineralogical, physical, chemical and geotechnical properties. The mudstones were pulverized by a standard grinding method frequently used in the production of powdered commercial bentonite.

3.2. Mineralogical, chemical and physicochemical characterization

Mineralogical analyses were carried out on oriented and random powder samples by means of X-ray diffraction (XRD) analysis, using a SIEMENS D-500 X-ray diffractometer with automatic slit and a Cu-Kα tube (at $\lambda = 1.5406$ Å, 40 kV, 30 mA). The semi-quantitative composition (%) of the samples was obtained in different ways for the identified mineral phases. Quartz and feldspars were quantified by XRD using the internal standard method, with ZnO as standard phase [25]. Zeolites were quantified by XRD through the construction of calibration curves for zeolite–mudstones mixtures using 0%, 2.5%, 5% and 10% of zeolite. Calcite and total carbonates contents were measured by the gasometric method in a Scheibler calcimeter. Semi-quantification of the identified clay minerals was done by calculating the ratio of the basal peak areas, after applying empirical correction factors on the peak areas [26,27].

Total carbon and sulphur analyses were performed in a LECO CS 230 analyser. Bulk chemical analyses were performed by ICP emission spectrometry (ICP-AES) following a lithium metaborate/tetraborate fusion and dilute nitric digestion.

The cation exchange capacities (CEC) of the samples was examined by measuring the Ag remaining in the solution after Ag–thiourea (Ag–Tu) extraction [28]. Silver and exchangeable cations were measured by atomic absorption spectrometry (AAS) in the extract which was used to saturate the sample.

External surface area was determined using a surface-area analyser (Asap 2000) by adsorption of nitrogen gas at 77 K, applying the BET equation (SS_{BET}). Specific surface area of the mudstones was also determined by conducting Ethylene Glycol Monoethyl Ether (EGME) absorption tests ($SS_{EGME)}$ [29]. The pH of aqueous dispersions of the mudstones (6.41×10^{-2}kg/L) was measured with a digital pH meter (Altronix TPX II).

3.3. Physical characterization

Grain-size analysis was determined by laser diffractometry using a particle size analyser (Cilas 1180L). A high-resolution LEO 1530 (Zeiss) scanning electron microscope (SEM) was used to study the structure of the mudstones.

Pore access size measurement was done by mercury injection porosimetry (MIP) using a Micrometrics AutoPore III 9420 porosimeter with 414 MPa maximum pressure, capable of measuring pores between 0.003 and 500 μm in diameter. Micropore size distributions of the mudstones (<100 Å) were examined by means of low-temperature N_2 sorption isotherms to saturation.

Atterberg limits were determined in accordance with the standard procedures outlined by ASTM D4318 [30]. These results were used to evaluate water–clay interactions given that liquid limit and plastic index depend on mineralogy and fluid chemistry [31–33].

Specific gravity was measured by the pyknometer method on clay air-dried at 105°C. Free swell tests were performed in accordance with ASTM D5890 [34].

Rheological properties were obtained according to the American Petroleum Institute Specification 13A for drilling fluids [35].

3.4. Hydraulic conductivity tests

Hydraulic conductivity of pure mudstones was determined from consolidation test performed by following the ASTM D2435 testing method [36]. Powdered mudstones were mixed with distilled water and placed in fixed-ring oedometer cells. An amount of water higher than the liquid limit was used in order to reach a saturation degree close to one when pouring the wet mixture in the cell. The following vertical pressures were applied to the specimens: 53.64, 107.28, 268.21, 536.52 and 1073 kPa.

Hydraulic conductivities were calculated by fitting Terzaghi's theory of consolidation to the measured time-settlement response at each effective vertical pressure [37].

Sand–mudstones mixtures (15% w/w) were prepared to determine the hydraulic performance of compacted liners in laboratory. The sand mainly comprised quartz and was classified as well-graded sand (SW) according to the Unified Soil Classification System. Obtained uniformity and curvatures coefficients were $Cu = 8$ and $Cc = 1.4$, respectively.

The sand–mudstones mixtures were allowed to hydrate for 24 h prior to being compacted. Compaction was performed using the Proctor Standard energy and following the ASTM D698 standard procedure [38]. The hydraulic conductivity of specimens compacted at the optimum moisture content was measured in flexible-wall permeameters by following the falling head method described in DIN 18130-1 standard [39]. The pressure of the permeating liquid in the inlet port was 3000 kg/m^2 and the cell or confining pressure was 6000 kg/m^2. These conditions resulted in a hydraulic gradient of approximately 30 (dimensionless). Hydraulic conductivity measurements were repeated at least two times.

4. Results and discussion

4.1. Mineralogical and chemical composition

Figure 3 displays representative XRD patterns of randomly oriented powders of bulk rock and oriented aggregates. The XRD analyses show that the dominant minerals are an R0 smectite/illite mixed layer (70–90% Sm) followed by calcite (10–30%) and illite (∼10%) (Table 1). The accessory minerals, whose total content is lower than 10% w/w, are kaolinite, quartz, feldspars and zeolites. The mineralogical analyses confirm the presence of expandable clay minerals but also a significant amount of calcite that may be unfavourable for the potential applications of the tested mudstones.

The quantitative chemical composition of the mudstones as determined from ICP analysis is presented in Table 2. The chemical composition indicates the presence of considerable amounts of silica and aluminium, which is in agreement with the obtained mineralogy. Iron values are slightly high for smectite-rich materials [40] and are related to the presence of impurities [41]. The amount of total carbon is highly related to the mineralogical composition. Therefore the CA sample, which has the highest

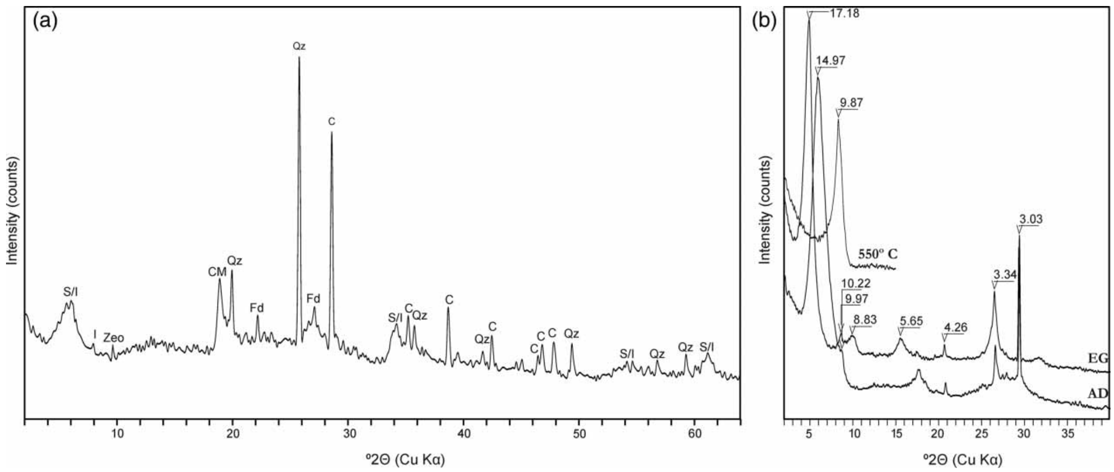

Figure 3. Representative X-ray patterns of calcareous mudstones (NTOL). a) Whole rock; b) <2 μm grain-size fraction, oriented samples. S/I: smectite/illite mixed layer; C: calcite; I: illite; Zeo: zeolites; Qz: quartz; Fd: feldspars; CM: clay minerals. AD: air-dried; EG: ethylene glycol solvated. The numbers represent basal spacings in Å.

Table 1. Mineral composition of mudstones (%).

Formation	Sample	S/I*	Illite	Kaolinite	Quartz	Feldspar	Calcite	Zeolites
Jagüel	CA	50–55	5–10	∼3	5 ± 1	<1	∼30	–
Roca	ETRO	65–70	∼10	<0, 5	7 ± 1	<1	10–15	–
	NTOL	∼70	∼10	–	7 ± 1	<1	∼10	∼2

*S/I = smectite/illite mixed layer.

Table 2. Chemical composition expressed in weight percent of oxides of bulk samples of the studied mudstones.

Formation	Sample	SiO_2 %	Al_2O_3 %	Fe_2O_3 %	MgO %	CaO %	Na_2O %	K_2O %	TiO_2 %	P_2O_5 %	MnO %	Cr_2O_3 %	Sr ppm	Zr ppm	Y ppm	C %	S %	L.O.I. %
Jagüel	CA	40.39	12.72	4.58	2.22	14.56	1.62	2	0.55	0.2	0.09	0	382	141	0	3.09	0.14	19.73
Roca	ETRO	50.72	13.49	5.04	2.79	6.58	2.01	1.92	0.58	0.11	0.05	0	225	125	0	1.47	0.20	16.47
	NTOL	50.58	15.02	5.98	2.6	3.36	2.08	2.7	0.64	0.23	0.09	228	238	164	64	1.19	0.06	16.9

CaO content (Table 2), has the highest percentage of total carbon in agreement with the calcite content shown in Table 1.

4.2. Physicochemical properties

Table 3 summarizes the CEC, individual exchangeable cations, and specific surface. The obtained values for amounts of Na^+ and Mg^{2+} are consistent with the marine origin of the mudstones. Properties determined for the NTOL and ETRO samples are in the expected range for smectite-rich sediments [42–44].

More than 50% of the exchange sites in CA and ETRO samples are occupied by Na^+, while in the NTOL sample Ca^{2+} is the main exchangeable cation (Table 3).

The specific surface determined by N_2 adsorption (SS_{BET}) showed quite low values as compared with that determined by using EGME (SS_{EGME}). This can be attributed to the fact that in the first case the specimen under test is in dry state, and then the inter-layer of the clays gets suppressed [45–47]. SS_{BET} values are consistent with other observations made on mixed-layer clay minerals [48–50]. Both specific surface values (SS_{BET} and SS_{EGME}) of the mudstones were high and similar to the values expected for natural bentonites, which indicates that the influence of smectite prevails over the other clay minerals.

The type and relative amounts of clay minerals and calcite in mudstones samples define the magnitude of CEC and SS_{EGME} values. Sample CA, which has the highest calcite content and lowest smectitic mixed-layer content, had the lowest CEC and SS_{EGME} values. However, the high specific surface and CEC obtained for the three tested mudstones suggest a good performance as adsorbent materials, since they are considerable higher than reported values for other mudstones from other parts of the world which are used as sorbents to attenuate containments in landfill liners (*i.e.* CEC: 22.1 cmol/kg, SS: 45 m^2/g) [51] (Table 3).

Table 3. Cation exchange capacity (CEC), exchangeable cations, and specific surface of mudstones.

Formation	Sample	CEC (cmol/kg)	Exchangeable cations (%)				Specific surface (m^2/g)	
			Ca^{2+}	Mg^{2+}	K^+	Na^+	S_{BET}	S_{EGME}
Jagüel	CA	52.17	20.54	14.63	1.68	63.16	56	548.71
Roca	ETRO	71.75	14.03	20.38	1.76	63.83	86	625.19
	NTOL	69.60	53.60	21.96	1.88	22.56	99	642.85

pH values are alkaline (CA: 9.67, NTOL: 8.97 and ETRO: 8.69), consistent with the measured calcite ($CaCO_3$) content.

4.3. Physical properties

The studied mudstones are massive, with evidence of a slight lamination when examined by means of direct visual observations. At low magnification (1000–3000×), the observed microfabric shows a close packing of randomly oriented individual clay particles (Figure 4(a)). The three specimens show significant amounts of calcareous nanofossils surrounded by clay flakes with edge-to-edge particle arrangements (Figure 4(b)). At higher magnification (8000×), clay flakes are arranged in edge-to-face and face-to-face contacts. These individual flakes form domains with randomly shaped voids. The morphology of the smectite/illite mixed layer (S/I) is slightly crenulated to flaky, and the mean diameter of individual particles is around 4 μm (Figure 4(e)). In Roca formation mudstones, a preferred particle orientation can be seen (Figures 4(c) and 4(d)). The texture is also closed, and is primarily controlled by the S/I particles arranged in face-to-face contacts and micropores in between with an elongated morphology parallel to the lamination (Figure 4(f)). In general, the pores observed under SEM have minimum and maximum sizes equal to 200 nm and 1 μm, respectively, and with a pattern typical of intra-aggregate pores [52–54].

The N_2 adsorption isotherms obtained for mudstones approach Type IIb [55], as shown in Figure 5. The hysteresis loops are of Type H3 in the IUPAC classification, with no indication of a plateau at high p/p_0 values and, therefore, no indication of the completion of mesopore filling. Such isotherms are given by either slit-shaped pores or, as in the present case, assemblages of platy particles such as the ones observed in the SEM pictures (Figures 4(e) and 4(f)).

Pore size distribution curves obtained by MIP can be seen in Figure 6. All the samples exhibit a porometric distribution characterized by the presence of one main type of pore with a diameter between 1–0.1 μm. Samples ETRO and CA also exhibit pores between 100–1000 μm. However, the existence of a certain Hg volume in this region would represent the breakdown of pores at higher pressure levels [56]. Many bottle-shaped pores are common in mudstones according to other Hg porosity studies [8]. Therefore, pore size ranges determined from mercury injection only refer to pore necks, which indeed is important when trying to find characteristic parameters for fluid displacement in porous media.

Pore structure properties determined by Hg porosimetry are in good agreement with the SEM observations, which also indicate the presence of pores smaller than 1 μm. A pore diameter between 3 and 8 μm is used as a boundary for the hydraulic flow [57]. However, in the case of fine soils and sediments, the hydraulic flow also depends on the thickness of the diffuse double layer, particle–fluid interaction mechanisms, and the presence and morphology of inter-aggregate pores [58–60].

Particle–fluid interaction can be inferred from Atterberg limits. The studied samples were classified as high plasticity silts (MH) and high plasticity clays (CH) according to the Unified Soil Classification System (Table 4). Grain-size analyses show that the mudstones are mainly composed of silt and clay particles. The grinding method provides in all cases very similar amounts of fine particles (clay and silt size). Almost all particles have a size lower than 62.5 μm, and the amount of clay size particles (<2 μm) is larger than 15% (Table 4). Based on the grain-size distribution and Atterberg limits, the activity of the samples falls into a range typical for mudstones according to the Skempton classification [61], and shows a good correlation with the mineralogy detected in the XRD tests (Table 4). In addition, specific gravity values were found to be very similar to that of smectite-rich clays [62]. The Atterberg limits, percentages of fines and activity of the mudstones meet with the standard specifications proposed for liner materials [63].

Free swell index is very low (< 10 mL) as a consequence of the presence of Ca^{2+} in the system (as an exchangeable cation or as a part of the calcite). In coincidence with this trend, the plastic viscosity of the mudstones was also considerably low, and controlled by the Ca^{2+} and the alkaline pH which determine particle association and rheology [64–66]. In an alkaline medium, particle arrangement is mainly face-to-face contacts (band-like structures) which would result in a poor capacity to form a gel in clay aqueous dispersions [67–70].

4.4. Hydraulic conductivity

4.4.1. Pure mudstones

The hydraulic conductivity values were between one and two orders of magnitude below the required value of

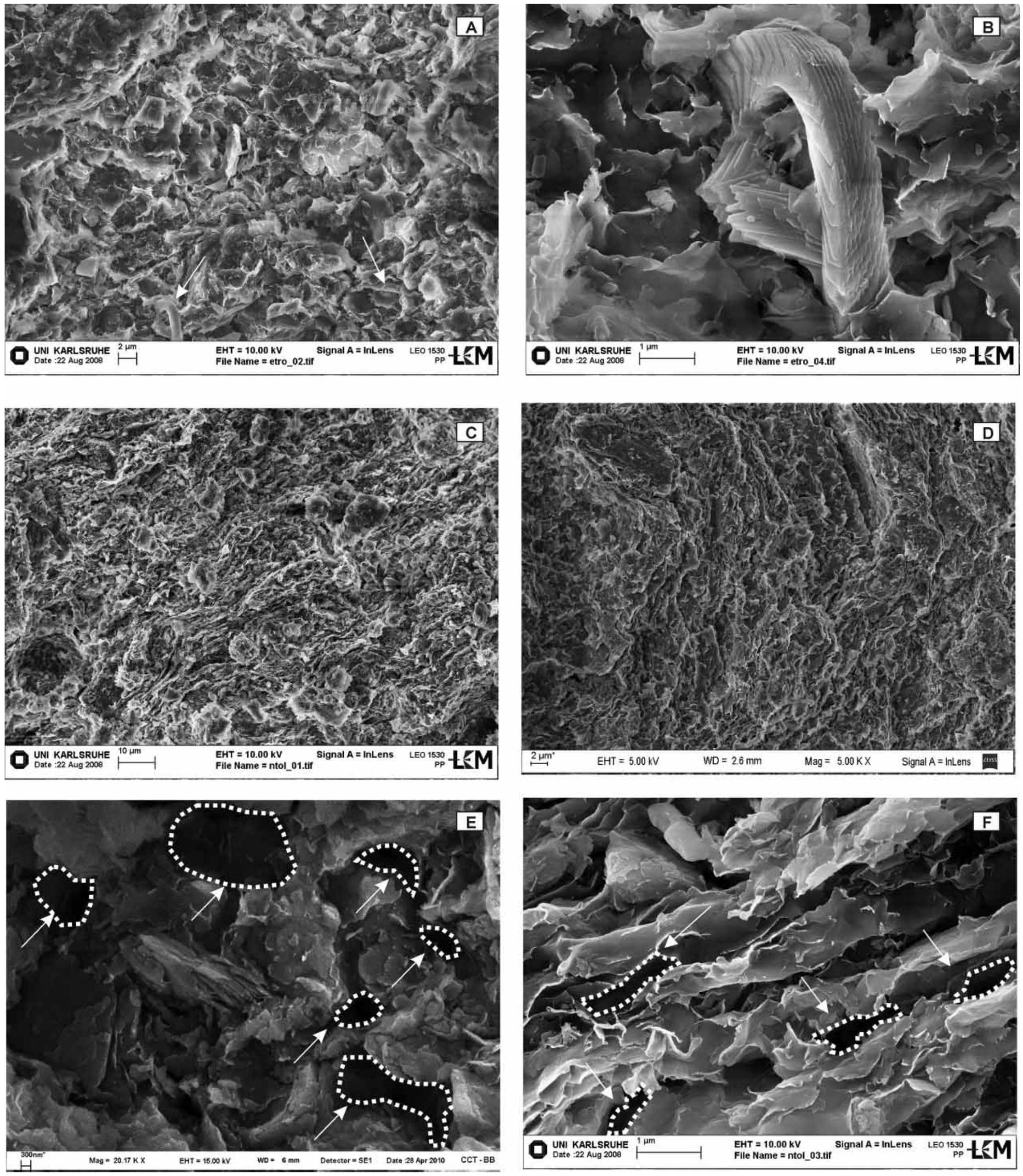

Figure 4. SEM images of Jagüel and Roca formations mudstones. (A) sample CA: randomly oriented particles of S/I, the arrows show calcareous nanofossils; (B) detail of a calcareous nanofossil rounded by clay flakes; (C) and (D) samples ETRO and NTOL respectively showing a close packing texture and a particle preferred orientation; (E) sample CA: arrows indicate intra-aggregate pores with an irregular to rounded shape; (F) sample NTOL: arrows indicate intra-aggregate pores with a planar shape.

1×10^{-09} m/s for clay liners. Figure 7 shows that the hydraulic conductivities of the tested mudstones are lower than 3.2×10^{-10} m/s and decrease significantly with the effective pressure. This trend can be attributed to the specimen consolidation and the decrease of void ratio when the effective vertical pressure increases. The amount of clay-sized particles ($<2.0\,\mu$m) clearly controlled the hydraulic conductivity as expected when the clay fraction is higher than 5% or 7% [60,71].

The hydraulic conductivities showed the same order of magnitude as the measured values of a Na-bentonite from North Patagonia, Argentina, even when the tested mudstones have very low intrinsic swelling [72]. These values compare well with those obtained for Mercia mudstone from the United Kingdom ($\sim 1 \times 10^{-10}$ m/s) and a mudstone from south-western Taiwan ($\sim 7 \times 10^{-10}$ m/s), which are both currently used as liners in environmental applications [73,74]. SEM, pore size distribution and grain-size analysis confirm that the mudstones largely consist of very small particles which define very thin flow channels as a result of the almost exclusive presence of micropores (intra-aggregate and inter-particle pores). The plasticity of

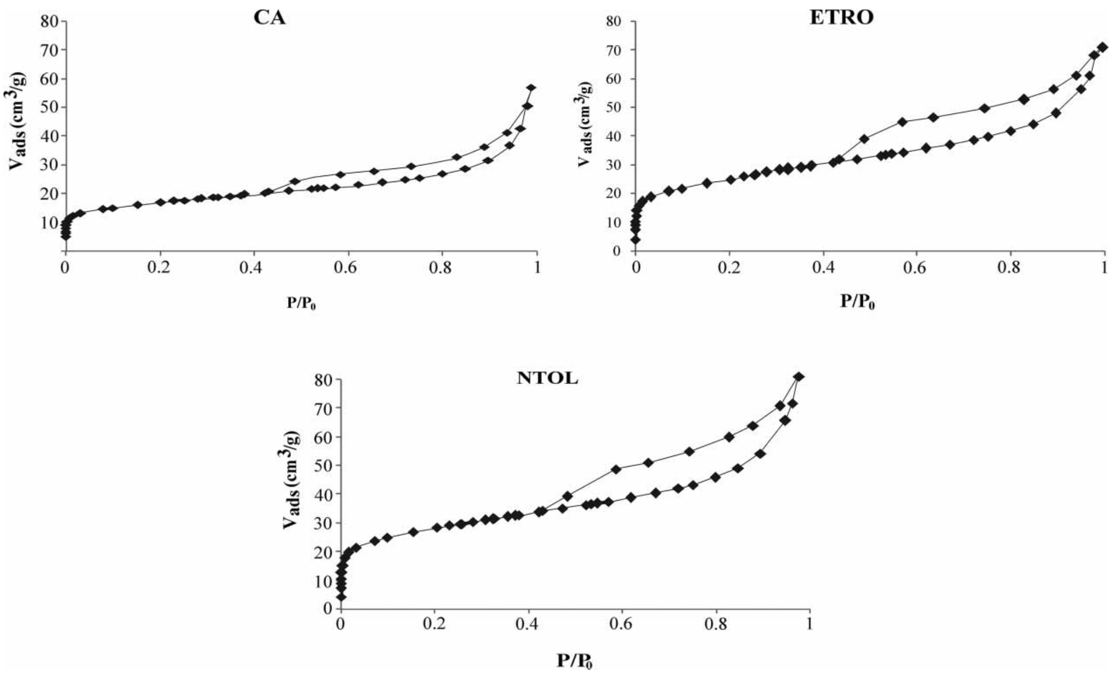

Figure 5. N_2-isotherms of the calcareous mudstones from Jagüel and Roca formations.

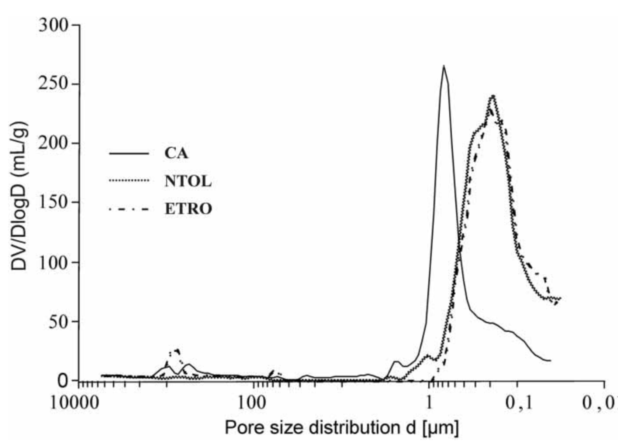

Figure 6. Pore size distributions obtained by mercury porosimetry.

Table 4. Main physical properties of tested mudstones.

	Jagüel	Roca	
Property	CA	ETRO	NTOL
Water content (%)	4.6	5.01	5.5
Liquid limit (%)	110	185	117
Plasticity index	54	120	52
Swell index (mL)	8	11	7
Specific gravity	2.63	2.65	2.64
Activity	0.94	2.36	1.70
Unified Soil Classification	MH	CH	MH
VP (Cps)	2	3	3
Particles $< 62.5\,\mu m$ (%)	100	100	99.85
Particles $< 3.9\,\mu m$ (%)	57.1	50.8	30.5
Particles $< 1.95\,\mu m$ (%)	34.2	28.3	17.69
Particles $< 0.98\,\mu m$ (%)	17.3	13.82	8.76

the samples indicates that particle–water interactions may be the main factor controlling the hydraulic conductivity of the mudstones. In general, the influence of plasticity on soil hydraulic properties can be predicted from the liquid limit, plasticity and void ratio [75].

Given that the mudstones have very low swelling capacity due to the carbonate content, the presence of exchangeable cations has negligible influence on the observed hydraulic conductivity. Therefore, mudstones would be chemically stable when used as barriers for waste leachates containing inorganic cations or organic liquids [1,31]. In high-swelling Na-bentonites, contact with concentrated salt solutions reduces the diffuse double layer thickness and raises the permeability [60,76–78]. In addition, these low-swelling mudstones, with low intrinsic permeability, would maintain greater cohesion on drying. This behaviour is very

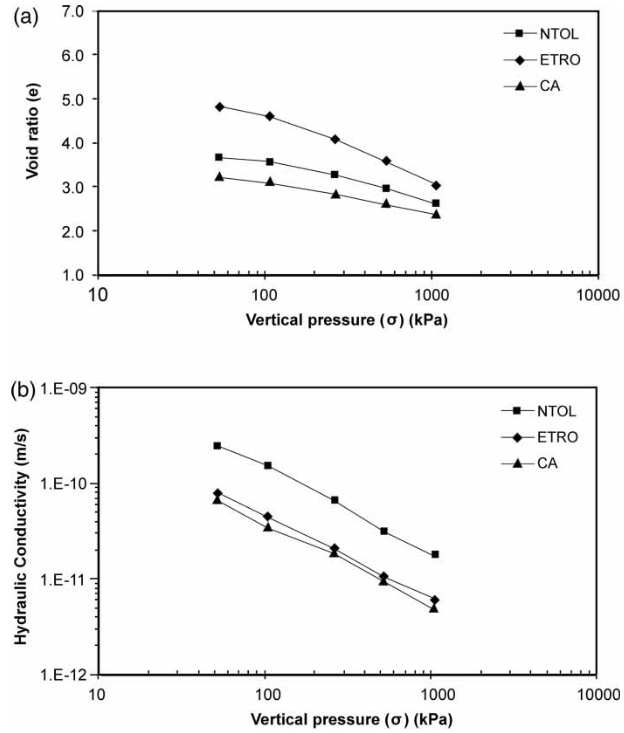

Figure 7. Hydraulic conductivity and void ratio of powdered mudstones vs. effective vertical pressures.

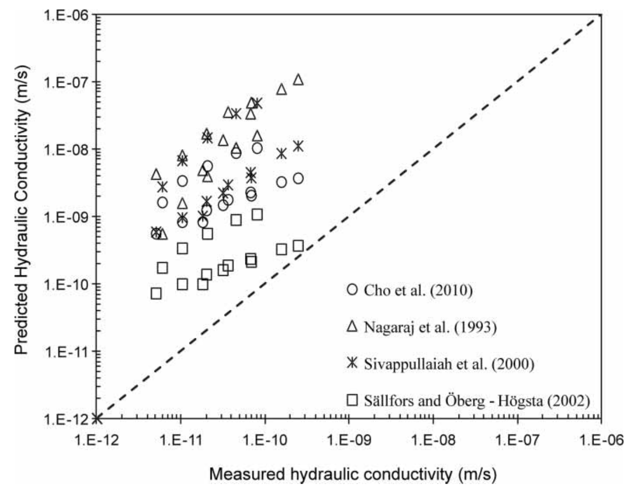

Figure 8. Observed and predicted hydraulic conductivities of mudstones samples at different void ratios.

favourable compared with a swelling bentonite, which is likely to crack when dry, thereby allowing easy water flow.

The range of vertical pressure imposed in these experiments (53.64–1073 kPa) represents overburden pressures exerted on clay liners used to seal hazardous waste landfills, sanitary landfills, waste piles and mining waste surface impoundments [79]. The experiments therefore simulate loads applied in landfill sites and other waste disposal sites requiring containment and minimum leakage.

4.4.2. Sand–mudstone mixtures

Table 5 shows the hydraulic conductivities of compacted sand–mudstone mixtures. The mean values measured ranged from 1.2×10^{-10} to 1.9×10^{-10} m/s (Table 5). Hydraulic conductivity of the sand was 5.67×10^{-4} m/s. However, the hydraulic conductivity of the mixtures was found to be similar to those measured for pure mudstones. Therefore, the hydraulic behaviour of the mixtures was controlled by the powdered mudstones. The particle arrangement as determined in the SEM analysis plays a fundamental role in governing the hydraulic conductivity of the compacted sand–mudstone mixtures [80]. The sand–mudstone mixtures had a hydraulic conductivity only one order of magnitude higher than an identical mixture using a Na-bentonite from this region [72].

Most of empirical formulations developed to predict the hydraulic conductivities of clay and clay–sand mixtures were developed for pure clays, frequently for bentonite. Thus, these models fail in predicting the hydraulic properties of mudstones given that measured hydraulic conductivities are fairly similar to those measured in bentonite but the plasticity index and liquid limit are significantly lower than those of a bentonite. Figure 8 presents a comparison between experimental results and the expected hydraulic conductivity computed according to different models reported in the literature. These models allow estimation of the hydraulic properties from void ratio (or dry unit weight), liquid limit and void ratio at liquid limit. In general, most of predictive models provide values from one to three orders of magnitude higher than the observed hydraulic conductivities of the mudstones [75,81–83] (Figure 8).

Results confirm that the mudstones have satisfactory hydraulic behaviour to be considered as construction materials for compacted clay liners. In particular, the mineralogical and chemical properties are compatible with the use of mudstones for the construction of compacted sand–mudstone covers and surface impoundments.

Table 5. Compaction properties and hydraulic conductivity (K) of sand-mudstone mixtures.

Formation	Sample	Optimum water content (%)	Dry density (kN/m^3)	K (m/s)	Standard deviation (m/s)
Jagüel	CA	12.5	18.9	1.9E-10	1.66E-11
Roca	ETRO	12	18.7	1.29E-10	2.41E-11
	NTOL	11.5	18.8	1.46E-10	1.64E-11

5. Conclusions

Calcareous mudstones from Jagüel and Roca formations from North Patagonia Argentina consist of a smectite/illite mixed layer and, to a lesser extent, calcite. The geotechnical and physicochemical behaviour of these materials mainly depends on particle arrangement, pore structure and mineralogical composition. The mudstones have a high external and total surface area and a significant amount of calcium, which reduce the expansion potential and plasticity.

The mudstones achieve very low hydraulic conductivity without swelling. Observed values were as low as those typically determined for a natural Na-bentonite from this region and are in accordance with hydraulic conductivities values obtained for mudstones from other parts of the world which are currently used as liners in environmental applications.

A face-to-face particle arrangement observed at microscale and a significant amount of clay-sized particles were the two main factors controlling the macroscopic hydraulic behaviour of the mudstones.

The pore size distribution, determined from mercury injection, N_2 sorption isotherms and SEM images, indicates that the mudstones are mainly constituted by ultra and micropores (intra-aggregates pores). However, liquid displacement inside pores is mainly controlled by the largest pore population or presence of macropores (inter-aggregates pores). The micropores, with a characteristic pore size and shape, are the ones which control the hydraulic properties of the mudstones.

The hydraulic properties of the mudstones and sand–mudstone mixtures are lower than the required value for liners and covers ($k < 10^{-9}$ m/s). However, sand–mudstone mixtures are easier to use in field applications. An important observation is that the observed hydraulic conductivities do not depend on swelling and the nature of the exchangeable cation. In this way, these mixtures could be used as a barrier to many contaminants because they would be more stable than bentonites. However, since this study evaluated their hydraulic conductivity to water, further studies involving hydraulic conductivity tests using salt solutions of different concentrations are recommended. These tests, in combination with sorption studies, would allow the evaluation of the long-term performance of these materials in contact with real leachates as well as their contaminant-attenuation capacity.

Calcareous mudstones from the Jagüel and Roca formations may be used for the construction of compacted soil barriers and for the isolation of many contaminants, given the significant presence of calcite that reduces the expected swelling. This indicates that barriers made from the studied mudstones should show minimal cracking on drying. Mudstones are very common in almost all the sedimentary basins in the world; therefore, the obtained results are fundamental when considering them as a low-cost geomaterial for environmental applications. Particularly, good performance is expected when they are used as a construction material for landfill covers and liners in surface impoundments in arid and semiarid climates, due to the low swelling of the tested materials.

Acknowledgements

The authors thank CONICET, SECyT-UNComa (project 04/I107) and the Agencia Nacional de Promoción Científica y Tecnológica (PICT 2002-07-12633) for the financial support of this research. The first author would like to thank to the laboratory of Surface Sciences and Porous Medium from Universidad Nacional de San Luis in Argentina for the N_2 sorption isotherms determinations.

References

[1] Churchman GJ, Askary M, Peter P, Wright M, Raven MD, Self PG. Geotechnical properties indicating environmental uses for an unusual Australian bentonite. Appl Clay Sci. 2002;20:199–209.
[2] Johnson B, Balserak P, Beaulieu S, Cuthbertson B, Stewart R, Truesdale R, Whitmore R, Young J. Industrial surface impoundments: environmental settings, release and exposure potential and risk characterization. Sci Total Environ. 2003;317:1–22.
[3] USEPA. Design, construction, and evaluation of clay liners for waste management facilities. Tech. Rep. EPAr530rSW-86r007, Cincinnati (OH); 1992.
[4] Kayabali K. Engineering aspects of a novel landfill liner material: bentonite amended natural zeolite. Eng Geol. 1997;46:105–114.
[5] Goldman LJ, Greenfield LI, Damle AS, Kingsbury GL, Northeim CM, Truesdale RS. Design, construction, and evaluation of clay liners for waste management facilities. Tech. Rep. USEPA, EPA/530/SW-89/007F, Washington (DC); 1998.
[6] DeSutter TM, Pierzynski GM. Evaluation of soils for use as liner materials: a soil chemistry approach. J Environ Qual. 2005;34:951–962.
[7] Chalermyanont T, Arrykul S, Charoenthaisong N. Potential use of lateritic and marine clay soils as landfill liners to retain heavy metals. Waste Manage. 2009;29:117–127.
[8] Hildenbrand A, Urai JL. Investigation of the morphology of pore space in mudstones—first results. Mar Petrol Geol. 2003;20:1185–1200.
[9] Aplin AC, Fleet AJ, Macquaker JHS, eds. Mud and mudstones: physical and fluid-flow properties. London (UK): Geological Society, Special Publications 158; 1999.
[10] Mazurek M, Lanyon GW, Vomvoris S, Gautschi A. Derivation and application of a geologic dataset for flow modeling by discrete fracture networks in low-permeability argillaceous rocks. J Contam Hydrol. 1998;35:1–17.
[11] Mazurek M, Gautschi A, Marschall P, Vigneron G, Lebon P, Delay J. Transferability of geoscientific information from various sources study sites, underground rock laboratories, natural analogues to support safety cases for radioactive waste repositories in argillaceous formations. Phys Chem Earth. 2008;33:95–105.
[12] Slizowski K, Janeczek J, Przewlocki K. Suitability of salt-mudstones as a host rock in salt domes for radioactive-waste storage. App Energ. 2003;75:119–128.
[13] Lin TT, Cheng CH. Microanalytical characterizations of eroded and slaked mudstone proposed as landfill liner material. Pract Period Hazard Toxic Radioact Waste Manage. 2006;10:128–133.

[14] Delage P, Cui YJ, Tang AM. Clays in radioactive waste disposal. J Rock Mechan Geotech Eng. 2010;2:111–123.
[15] Fityus SG, Smith DW. The development of a residual soil profile from a mudstone in a temperate climate. Eng Geol. 2004;74:39–56.
[16] Yang Y, Aplin AC. A permeability–porosity relationship for mudstones. Mar Petrol Geol. 2010;278:1692–1697.
[17] Groeber P. Observaciones geológicas a lo largo del meridiano 70°. Hoja Chos Malal Rev Asoc Geol Arg. 1946;1: 177–208.
[18] Legarreta L, Gulisano CA. Análisis estratigráfico secuencial de la cuenca Neuquina Triásico superior – Terciario inferior; Argentina. In: Chebli GA, Spalletti LA, editors. Cuencas Sedimentarias Argentinas, serie de correlación geológica. Tucumán (Argentina); 1989. p. 221–244.
[19] Uliana M, Dellapé D. Estratigrafía y evolución paleoambiental de la sucesión Maastrichtiano-Eoterciaria del engolfamiento neuquino Patagonia Septentrional.; Actas 8° Congreso Geológico Argentino, Buenos Aires. 1981;3: 673–711.
[20] Musso TB, Concheyro A, Pettinari G. Mineralogía de arcillas y nanofósiles calcáreos de las formaciones Jagüel y Roca en el sector oriental del lago Pellegrini, cuenca Neuquina, República Argentina. Andean Geol. 2012;393:511–540.
[21] Andreis R, Iñíguez Rodríguez A, Lluch J, Sabio D. Estudio sedimentológico de las formaciones del Cretácico superior del área del Lago Pellegrini provincia de Río Negro, República Argentina. Rev Asoc Geol Arg. 1974;291: 85–104.
[22] Bertels A. Estratigrafía del límite Cretácico-Terciario en la Patagonia septentrional. Rev Asoc Geol Arg. 1969;XXIV:41–54.
[23] Espejo PM, Nieto DG. Geología y Recursos Minerales del sector Rionegrino de las Hojas 3769-IV, Catriel; 3969-II, Neuquén; 3966-I, Gobernador Duval; 3966-II, Puelches y 3963-I, Río Colorado. Tech. Rep. Dirección de Minería de Río Negro-SEGEMAR. Viedma (Argentina); 1999.
[24] Hugo CA, Leanza HA. Hoja Geológica 3969-IV, General Roca. Provincias de Río Negro y Neuquén. Tech. Rep. Instituto de Geología y Recursos Minerales. Buenos Aires (Argentina): Servicio Geológico Minero Argentino; 2001.
[25] Hardy M. X-ray diffraction measurement of the quartz content of clay and silt fractions in soils. Clay Miner. 1992;27:47–55.
[26] Jones R. A computer technique for X-ray diffraction curve fitting/peak decomposition, in quantitative mineral analysis of clays. In: Pevear DR, Mumpton FA, editors. CMS Workshop Lectures. Evergreen (CO): Clay Minerals Society; 1989, p. 51–101.
[27] Schwertmann U, Niederbudde E. Tonminerale in Böden, In: Jasmund K, Lagaly G, editors. Tonminerale und Tone. Darmstadt (Germany): Steinkopff Verlag; 1993, p. 212–265.
[28] Dohrmann R, Echle W. Eine kritische Betrachtung der Silber-Thioharnstoff-Methode AgTu) zur Bestimmung der Kationenaustauschkapazitaet und Vorstellung eines neuen methodischen Ansatzes. In: Kohler EE, editor. Berichte der deutschen Ton- un tonmineralgruppe, Regensburg; 1994, p. 213–222.
[29] Carter DL, Heilman MD, Gonzalez CL. Ethylene glycol monoethylether for determining surface area of silicate minerals. Soil Sci. 1965;100:356–360.
[30] ASTM Standard D4318. Standard test method for liquid limit, plastic limit and plasticity index of soils. West Conshohocken (PA): ASTM International; 2005. www.astm.org
[31] Gleason MH, Daniel D, Eykholt GR. Calcium and sodium bentonite for hydraulic containment applications. J Geotech Geoenviron. 1997;1235:438–445.
[32] Candelaria LM, Matsumoto MR. Effects of NAPL contaminants on the permeability of a soil–bentonite slurry wall material. Transport Porous Med. 2000;381–382:43–56.
[33] Schmitz RM, Schroeder C, Charlier R. Chemo-mechanical interactions in clay: a correlation between clay mineralogy and Atterberg limits. Appl Clay Sci. 2004;26: 351–358.
[34] ASTM Standard D5890. Standard test method for swell index of clay mineral component of geosynthetic clay liners. West Conshohocken (PA): ASTM International; 2006. www.astm.org
[35] API 1993 API Specification 13A. Specification for drilling-fluid materials, 15th edn. Northwest Washington: American Petroleum Institute.
[36] ASTM Standard D2435. Standard test methods for one-dimensional consolidation properties of soils using incremental loading. West Conshohocken (PA): ASTM International; 2011. www.astm.org
[37] Mesri G, Olson R. Mechanisms controlling the permeability of clays. Clay Clay Miner. 1971;19:151–158.
[38] ASTM Standard D698. Standard test methods for laboratory compaction characteristics of soil using standard effort 12 400 ft-lbf/ft^3 600 kN-m/m^3. West Conshohocken (PA): ASTM International; 2011. www.astm.org
[39] DIN 18130-1. Soil, investigation and testing — determination of the coefficient of water permeability. Part 1: laboratory tests. Bauwesen NABau im DIN, Deutsches Institut für Normung e.V., Berlin: Beuth; 1998.
[40] Stucki JW, Kostka JE. Microbial reduction of iron in smectite. Comptes Rendus Geoscience. 2006;338:468–475.
[41] Musso TB. Minerales arcillosos de la región Norpatagónica para ser usados como barreras impermeables en la disposición de residuos. [PhD dissertation]. Río Cuarto (Argentina): Universidad Nacional de Río Cuarto; 2011.
[42] Keijzer TJS, Kleingeld PJ, Loch JPG. Chemical osmosis in compacted clayey material and the prediction of water transport. J Eng Geol. 1999;53:151–159.
[43] Triantafyllou S, Christodoulou E, Neou-Syngouna P. Removal of nickel and cobalt from aqueous solutions by Na-activated bentonite. Clay Clay Miner. 1999;475: 567–572.
[44] Shackelford CD, Lee JM. The destruction role of diffusion on clay membrane behavior. Clay Clay Miner. 2003;512: 186–196.
[45] Aylmore LAG, Quirk JP. The micropore size distributions of clay mineral systems. J Soil Sci. 1967;181:1–17.
[46] Santamarina JC, Klein KA, Wang YH, Prencke E. Specific surface area: determination and relevance. Can Geotech J. 2002;39:233–241.
[47] Arnepalli DN, Shanthakumar S, Hanumantha B, Singh D. Comparison of methods for determining specific-surface area of fine-grained soils. Geotech Geol Eng. 2008;26: 121–132.
[48] Srasra E, Bergaya F, Fripiat JJ. Infrared spectroscopy study of tetrahedral and octahedral substitutions. Interstratified illite-smectite clay. Clay Clay Miner. 1994;423:237–241.
[49] Omotoso OE, Mikula RJ. High surface areas caused by smectitic interstratification of kaolinite and illite in Athabasca oil sands. Appl Clay Sci. 2004;25:37–47.
[50] Villegas AS, Santo JL, Mattos M, Aguiar M, Guarino A. Characterization of natural brazilian clays and their utilization as catalysts in the coiodination of alkenes with water and alcohols. J Braz Chem Soc. 2005;163B:565–570.
[51] Stringfellow AM, Simoes A, Smallman D, Beaven R, Powrie W, Potter HAB. Sorption of Mecoprop by two clay landfill liner materials: Oxford clay and Mercia Mudstone. Q J Eng Geol Hydrogeol. 2011;44:321–329.

[52] Pusch R, Karlnland O, Hokmark H. GMM-a general microstructural model for qualitative and quantitative studies of smectite clays. Tech. Rep. Stockholm (Sweden): SKB; 1990.
[53] Yong R. Overview of modeling of clay microstructure and interactions for prediction of waste isolation barrier performance. Eng Geol. 1999;54:83–91.
[54] Delage P, Marcial D, Cui YJ, Ruiz X. Ageing effects in a compacted bentonite: a microstructure approach. Geotechnique. 2006;565:291–304.
[55] Rouquerol J, Avnir D, Fairbridge C, Everett D, Haynes J, Pernicone N, Ramsay J, Sing K, Unger K. Recommendations for the characterization of porous solids. International Union of Pure And Applied Chemistry. Pure & Appl Chem. 1994;668:1739–1758.
[56] Dullien FAL. Porous media: fluid transport and pore structure. New York (NY): Academic Press; 1979.
[57] Busch KL, Luckner L. Geohydraulik. – 2, Aufl. Leipzig (Germany): VEB Deutscher Verlag für Grundstoffindustrie; 1973.
[58] Garcia-Bengochea L, Altschaeffl AG, Lovellm CW. Pore distribution and permeability of silty clays. J Soil Mech Foun Div ASCE. 979;1057:839–856.
[59] Schmitz RM. Can the diffuse double layer theory describe changes in hydraulic conductivity of compacted clay? Geotech Geol Eng. 2006;24:1835–1844.
[60] Montoro M, Francisca F. Soil permeability controlled by particle-fluid interaction. Geotech Geol Eng. 2010;28:851–864.
[61] Perloff WH, Baron W. Soil mechanics: principles and applications. New York (NY): John Wiley and Sons; 1976.
[62] Alawaji H. Swell and compressibility characteristics of sand–bentonite mixtures inundated with liquids. Appl Clay Sci. 1999;15:411–430.
[63] Daniel DE. Geotechnical practice for waste disposal. London (UK): Chapman and Hall; 1993.
[64] van Olphen H. An introduction to clay colloid chemistry, 2nd ed. New York (NY): Wiley; 1977.
[65] de Kretser RG, Scales PJ, Boger DV. Surface chemistry-rheology inter-relationships in clay suspensions. Colloids Surf, A Physicochem Eng Asp. 1998;137:307–318.
[66] Lagaly G, Ziesmer S. Colloid chemistry of clay minerals: the coagulation of montmorillonite dispersions. Adv Colloid Interface Sci. 2003;100–102:105–128.
[67] Lagaly G. Principles of flow of kaolin and bentonite dispersions. Appl Clay Sci. 1989;4:105–123.
[68] Permien T, Lagaly G. The rheological and colloidal properties of bentonite dispersion in the presence of organic compounds IV. Sodium montmorillonite and acids. Appl Clay Sci 1994a;9:251–263.
[69] Permien T, Lagaly G. The rheological and colloidal properties of bentonite dispersion in the presence of organic compounds III. The effect of alcohols on the coagulation of sodium montmorillonite. Colloid Polym Sci. 1994b;272:1306–1312.
[70] Palomino A, Santamarina JC. Fabric map for kaolinite: Effects of pH and ionic concentration on behaviour. Clays Clay Miner. 2005;533:211–223.
[71] Santamarina JC, Klein KA, Fam MA. Soils and waves. Chichester (UK): John Wiley & Sons; 2001.
[72] Musso TB, Roehl KE, Pettinari G, Valles J. Assesment of smectite-rich claystones from Northpatagonia for their use as liner materials in landfills. Appl Clay Sci. 2010; 83:438–445.
[73] Murray EJ, Davis J, Keeton P, Hill RG. Laboratory permeability measurements with Mercia Mudstone. In: Yong RN, Thomas HR, editors. Geoenvironmental engineering geoenvironmental impact management. London (UK): Thomas Telford Ltd., 2001; p. 455–463.
[74] Sheu C, Lin TT, Chang JE, Cheng CH. The feasibility of mudstone material as a natural landfill liner. J Hazard Mater. 1998;58:237–247.
[75] Nagaraj TS, Pandian NS, Narasimha Taju PSR. Stress state – permeability relationships for fine-grained soils. Geotechnique. 1993;4329:333–336.
[76] Petrov R, Rowe R. Geosynthetic Clay Liner (GCL) – Chemical compatibility by hydraulic conductivity testing and factors impacting its performance. Can Geotech J. 1997;34:863–885.
[77] Jo HY, Katsumi T, Benson CH, Edil TB. Hydraulic conductivity and swelling of nonprehydrated GCLs permeated with single-species salt solutions. J Geotech Geoenviron. 2001;1277:557–567.
[78] Lee JM, Shackelford CD. Impact of bentonite quality on hydraulic conductivity of geosynthetic clay liners. J Geotech Geoenviron. 2005;1311:64–77.
[79] Peirce JJ, Sallfors G, Murray L. Overburden pressures exerted on clay liners. J Environ Eng-ASCE. 1986;112:280–291.
[80] Mitchell J, Hooper D, Campanella R. Permeability of compacted clay. J Soil Mech Found Div ASCE. 1965;914:41–65.
[81] Cho WJ, Lee JO, Kwon S. Analysis of thermo–hydro–mechanical process in the engineered barrier system of a high-level waste repository. Nucl Eng Des. 2010;240:1688–1698.
[82] Sällfors G, Öberg-Högsta A. Determination of hydraulic conductivity of sand-bentonite mixtures for engineering purposes. Geotech Geol Eng. 2002;201:65–80.
[83] Sivapullaiah PV, Sridharan A, Stalin VK. Hydraulic conductivity of bentonite–sand mixtures. Can Geotech J. 2000;372:406–413.